

Article

Identification of *Daphne genkwa* and Its Vinegar-Processed Products by Ultraperformance Liquid Chromatography–Quadrupole Time-of-Flight Mass Spectrometry and Chemometrics

Hongying Mi ^{1,2}, Ping Zhang ^{2,*}, Lingwen Yao ², Huiyuan Gao ^{1,*}, Feng Wei ² , Tulin Lu ³ and Shuangcheng Ma ²

¹ School of Traditional Chinese Medicine, Shenyang Pharmaceutical University, Shenyang 110016, China

² Research and Inspection Center of Traditional Chinese Medicine and Ethnic Medicine, National Institutes for Food and Drug Control, National Medical Products Administration, No. 31 Huatuo Road, Beijing 102629, China

³ School of Chinese Material Medica, Nanjing University of Chinese Medicine, No. 138 Xianlin Road, Nanjing 210023, China

* Correspondence: zhangping@nifdc.org.cn (P.Z.); sypugaohy@163.com (H.G.); Tel.: +86-10-5385-2099 (P.Z.); Fax: +86-024-4352-0781 (H.G.)



Citation: Mi, H.; Zhang, P.; Yao, L.; Gao, H.; Wei, F.; Lu, T.; Ma, S. Identification of *Daphne genkwa* and Its Vinegar-Processed Products by Ultraperformance Liquid Chromatography–Quadrupole Time-of-Flight Mass Spectrometry and Chemometrics. *Molecules* **2023**, *28*, 3990. <https://doi.org/10.3390/molecules28103990>

Academic Editor: Victoria Samanidou

Received: 7 March 2023

Revised: 4 May 2023

Accepted: 4 May 2023

Published: 9 May 2023



Copyright: © 2023 by the authors. Licensee MDPI, Basel, Switzerland. This article is an open access article distributed under the terms and conditions of the Creative Commons Attribution (CC BY) license (<https://creativecommons.org/licenses/by/4.0/>).

Abstract: Crude herbs of *Daphne genkwa* (CHDG) are often used in traditional Chinese medicine to treat scabies baldness, carbuncles, and chilblain owing to their significant purgation and curative effects. The most common technique for processing DG involves the use of vinegar to reduce the toxicity of CHDG and enhance its clinical efficacy. Vinegar-processed DG (VPDG) is used as an internal medicine to treat chest and abdominal water accumulation, phlegm accumulation, asthma, and constipation, among other diseases. In this study, the changes in the chemical composition of CHDG after vinegar processing and the inner components of the changed curative effects were elucidated using optimized ultrahigh-performance liquid chromatography coupled with quadrupole time-of-flight mass spectrometry (UPLC-Q-TOF-MS). Untargeted metabolomics, based on multivariate statistical analyses, was also used to profile differences between CHDG and VPDG. Eight marker compounds were identified using orthogonal partial least-squares discrimination analysis, which indicated significant differences between CHDG and VPDG. The concentrations of apigenin-7-O- β -D-methylglucuronate and hydroxygenkwanin were considerably higher in VPDG than those in CHDG, whereas the amounts of caffeic acid, quercetin, tiliroside, naringenin, genkwanines O, and orthobenzoate 2 were significantly lower. The obtained results can indicate the transformation mechanisms of certain changed compounds. To the best of our knowledge, this study is the first to employ mass spectrometry to detect the marker components of CHDG and VPDG.

Keywords: *Daphne genkwa*; vinegar processing; medicinal component analysis; UPLC-Q-TOF-MS; chemometrics; potential quality marker compounds

1. Introduction

Chinese herbal medicines are processed following a unique pharmacological technology wherein crude drugs are treated in accordance with traditional Chinese medical theory by considering their individual nature and the requirements of drug dispensing, pharmaceutical preparation, and clinical use [1]. As a distinguishing characteristic of ancient pharmaceutical technology, traditional Chinese medicine (TCM) processing involves various techniques, including cleaning, cutting, roasting, steaming, and boiling, which significantly reduce toxicity or side effects, relieve drug irritation, enhance the therapeutic effects, and increase the clinical applicability of the extracts [2–4]. Among these techniques, stir-baking with excipients and frying with liquid excipients are regarded as the most effective and common processing methods [5]. Complex chemical changes occur during

herbal processing, thereby producing chemical constituents that may be the source of the clinical efficacy of the extract [6]. Therefore, the scientific mechanisms underlying this processing procedure should be clarified.

Daphne genkwa (DG) Sieb. et Zucc. (Thymelaeaceae) is an oriental herb widely distributed throughout China. Genkwa Flos, the dried flower buds of DG, is commonly used in TCM as an antitussive, expectorant, diuretic [7], antitumor [8,9], antileukemic [10], and anti-inflammatory [11,12] medicine. Crude herbs of DG (CHDG) are often used as an external medicine to treat scabies baldness, carbuncles, and chilblain owing to their significant purgation and curative effects. Vinegar-processed DG (VPDG) herbs are typically used as internal medicines to treat water swelling, chest and abdominal water accumulation, phlegm accumulation, qi inverse cough, asthma, and constipation, among other diseases. Various components have been identified in DG, including flavonoids [13,14], daphnane-type diterpene esters [15–17], lignans, coumarins, and amides [18,19]. Many complex chemical reactions occur during processing, such as hydrolysis, oxidation, displacement, isomerization, and decomposition, leading to changes in the clinical efficacy of DG. Therefore, determining the changes in the chemical composition of CHDG after processing and elucidating the cause of the changed curative effects are essential. Research into the medicinal properties of DG is mainly focused on chemical composition identification [20,21], quality control analysis [22,23], pharmacodynamic and toxicological evaluation [24–26], and pharmacokinetic studies [27,28]. In contrast, few studies have combined TCM processing with changes in the chemical composition of DG. Therefore, identifying the changes in the chemical compositions of DG after processing, and elucidating the underlying mechanisms that lead to these changes are valuable steps toward uncovering the secrets of traditional processing of Chinese medicinal herbs.

Liquid chromatography coupled with quadrupole time-of-flight mass spectrometry (UPLC-Q-TOF-MS) is widely employed owing to its high resolution, sensitivity, simplicity, and high throughput [29,30]. This technique has been successfully used for the analysis and identification of numerous types of compounds, including parent compounds and their metabolites, even at low concentrations [31]. In this study, a comprehensive comparison of CHDG and VPDG was conducted using UPLC-Q-TOF-MS to rapidly detect and identify the components in DG. Additionally, a multivariate statistical analysis approach was established to identify the changes in the chemical composition of CHDG caused by vinegar processing. These compositional changes can be used as potential markers in the quality control of CHDG and VPDG. Moreover, our study serves as a theoretical basis to explain the molecular-level mechanisms underlying the processing procedure.

2. Results and Discussion

2.1. Optimization of Chromatographic Separation and Mass Spectrometric Detection

The chromatographic conditions, including the mobile phase, flow rate, column, and temperature, were optimized to obtain good separation and strong responses from the numerous compounds in CHDG and VPDG. The ACQUITY HSS T3 (100 mm × 2.1 mm, 1.8 μm) analytical column was the most efficient for the separation at a column temperature of 30 °C. A solvent system of acetonitrile/water (0.1% formic acid) with gradient elution afforded high resolution and substantially few matrix interferences and was therefore used for the separation of the samples.

A previous study on the mass spectrometry (MS) analysis of DG [22] established that the negative ion mode yields the most spectral information and afforded a comprehensive method for the detection of components. A collision energy of between 20 and 60 eV provided an adequate number of fragments for structural analysis and was therefore selected as the optimal collision energy. Other MS parameters, including turbo-spray temperature, nebulizer gas, curtain gas, heater gas, ion spray voltage, and declustering potential, were also optimized to improve the response.

2.2. UPLC-Q-TOF-MS/MS Analysis and Identification of the Chemical Components of CHDG and VPDG

Using the optimized chromatographic and MS conditions, 67 components were identified, or tentatively characterized, in the negative ion mode after matching with the established UNIFI database or via reference standards and the published literature. Typical total ion chromatograms (TICs) of CHDG and VPDG in the negative ion mode are shown in Figure 1. The retention times, molecular formulas, ion types, detected masses, mass errors, and fragment ions associated with the identified peaks are summarized in Table 1. The constituents identified in DG were mainly classified as flavonoids, daphnane-type diterpene esters, lignans, coumarins, or others. The procedures to identify the major compounds (excluding “others”) are summarized as follows.

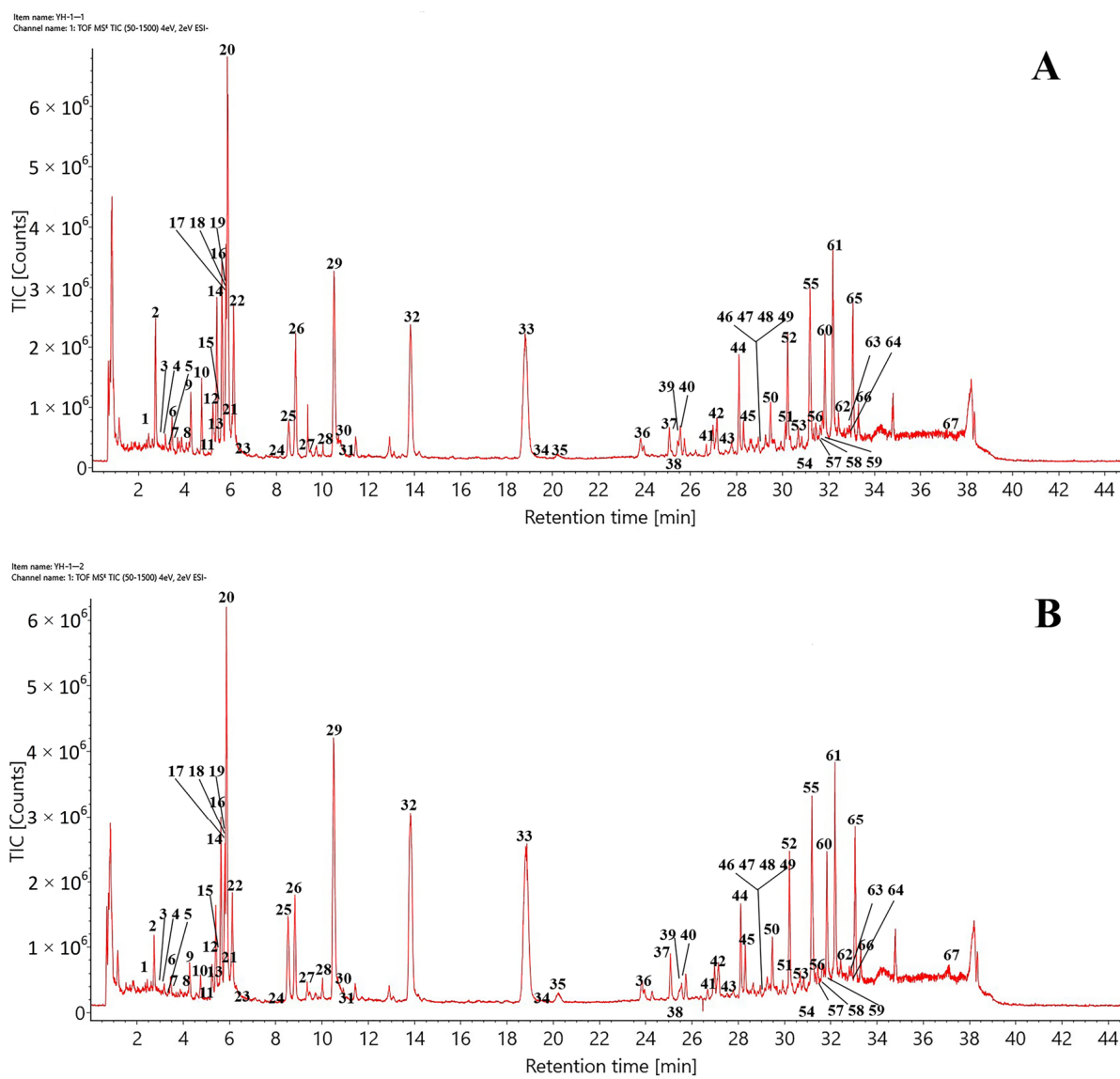


Figure 1. Typical TICs of (A) CHDG and (B) VPDG in the ESI[−] mode.

Table 1. Identification of chemical compounds via UPLC/Q-TOF-MS/MS.

No.	Retention Time, T_R (min)	Compound Name	Molecular Formula	Detected Mass (m/z)	Ion Type	Mass Error (ppm)	MS/MS (m/z)
1 *	2.43	protocatechuic acid	C ₇ H ₆ O ₄	153.0199	[M-H] ⁻	3.6	135.0258; 109.0292
2 *	2.74	chlorogenic acid	C ₁₆ H ₁₈ O ₉	353.0882	[M-H] ⁻	1.2	191.0567; 179.0345; 161.0245; 135.0451
3 *	2.86	rutin	C ₂₇ H ₃₀ O ₁₆	609.1461	[M-H] ⁻	-0.1	285.0393
4 *	3.21	isoquercitrin	C ₂₁ H ₂₀ O ₁₂	463.0879	[M-H] ⁻	-0.5	301.0353
5 *	3.32	pinoresinol diglucoside	C ₃₂ H ₄₂ O ₁₆	727.2454	[M-H+HCOOH] ⁻	-0.1	681.2395; 357.1347; 151.0393
6 *	3.37	caffein acid	C ₉ H ₈ O ₄	179.0354	[M-H] ⁻	2.1	135.0451
7	3.77	eleutheroside E	C ₃₄ H ₄₆ O ₈	787.2659	[M-H+HCOOH] ⁻	-1	417.1547; 367.1021; 181.0510
8	3.78	methyl 4-caffeylquinate	C ₁₇ H ₂₀ O ₉	367.1936	[M-H] ⁻	0.5	191.0559; 181.0510
9 *	4.28	cynaroside	C ₂₁ H ₂₀ O ₁₁	447.0929	[M-H] ⁻	-0.9	285.0403; 133.0293; 107.0131
10	4.74	apigenin-5-O- β -D-primeveroside	C ₂₆ H ₂₈ O ₁₄	563.1403	[M-H] ⁻	-0.6	311.0552; 269.0483; 117.0342
11 *	5.07	7-hydroxycoumarin	C ₉ H ₆ O ₃	161.0245	[M-H] ⁻	0.5	133.0311
12 *	5.23	luteolin-7-O- β -D-glucuronide	C ₂₁ H ₁₈ O ₁₂	461.0726	[M-H] ⁻	0	285.0403; 243.0286; 151.0036; 133.0296
13 *	5.28	kaempferol-3-O-glucosyl(1-2)rhamnoside	C ₂₇ H ₃₀ O ₁₅	593.1513	[M-H] ⁻	0.2	299.0563; 284.0326
14 *	5.4	genkwanin-5-O- β -D-glucoside	C ₂₁ H ₂₀ O ₁₀	431.0986	[M-H] ⁻	0.5	311.0562; 269.0459; 240.0423; 117.0347
15 *	5.57	apigenin-7-O- β -D-methylglucuronate	C ₂₂ H ₂₀ O ₁₁	505.0988	[M-H+HCOOH] ⁻	0.1	311.0562; 283.0613; 269.9452; 117.0347
16	5.63	hydroxygenkwanin-3'-O- β -D-glucoside	C ₂₂ H ₂₀ O ₁₁	461.1088	[M-H] ⁻	-0.3	284.0329; 255.0299; 133.0294
17 *	5.67	hydroxygenkwanin-5-O- β -D-glucoside	C ₂₂ H ₂₀ O ₁₁	461.1088	[M-H] ⁻	-0.3	284.0329; 255.0299; 133.0294
18 *	5.77	isovitexin	C ₂₁ H ₂₀ O ₁₀	477.1031	[M-H+HCOOH] ⁻	-1.5	271.0238; 117.0343
19	5.8	quercitrin	C ₂₁ H ₂₀ O ₁₁	447.0931	[M-H] ⁻	-0.3	284.0326
20	5.88	genkwanin-5-O- β -D-primveroside	C ₂₇ H ₃₀ O ₁₄	577.1566	[M-H] ⁻	0.6	283.0616; 269.0459; 268.0380; 175.0249
21	6.07	apigenin-7-O- β -D-glucuronate	C ₂₁ H ₁₈ O ₁₁	445.0777	[M-H] ⁻	0.1	269.0459; 175.0249; 113.0244
22	6.07	genkwanol A	C ₃₀ H ₂₂ O ₁₀	541.1144	[M-H] ⁻	0.6	417.0973; 285.0396; 227.0346
22	6.11	genkwanin-5-O- β -D-glucopyranoside	C ₂₃ H ₂₆ O ₉	445.1139	[M-H] ⁻	0.1	283.0631; 268.0390; 239.0374; 165.0200; 151.0034; 117.0342
23 *	6.28	quercetin	C ₁₅ H ₁₀ O ₇	301.0355	[M-H] ⁻	0.6	149.0240
24	7.94	edgeworthin	C ₁₈ H ₁₀ O ₇	337.0353	[M-H] ⁻	-0.3	164.0062; 112.9884
25 *	8.53	luteolin	C ₁₅ H ₁₀ O ₆	285.0405	[M-H] ⁻	0.1	151.0041; 133.0294
26 *	8.90	tiliroside	C ₃₀ H ₂₆ O ₁₃	593.1298	[M-H] ⁻	-0.4	447.0920; 307.0822; 285.0398; 227.0348; 211.0392; 145.0293; 117.0339
27	9.47	matairesinol	C ₂₀ H ₂₂ O ₆	357.1344	[M-H] ⁻	0.1	285.0434; 255.0264; 227.0343
28	9.69	naringenin	C ₁₅ H ₁₂ O ₅	271.0611	[M-H] ⁻	-0.5	255.0334; 151.0039
29 *	10.5	apigenin	C ₁₅ H ₁₀ O ₅	269.0460	[M-H] ⁻	1.6	117.0348; 107.0136
30 *	10.58	daphnoretin	C ₁₉ H ₁₂ O ₇	351.0513	[M-H] ⁻	0.9	190.9986; 163.0038; 135.0093
31	10.77	8-methoxykaempferol	C ₁₆ H ₁₂ O ₇	315.0510	[M-H] ⁻	0	300.0274
32 *	13.82	hydroxygenkwanin	C ₁₆ H ₁₂ O ₆	299.0562	[M-H] ⁻	0.4	284.0325; 256.0368; 227.0342; 151.0031; 133.0293
33 *	18.81	genkwanin	C ₁₆ H ₁₂ O ₅	283.0616	[M-H] ⁻	1.5	268.0378; 240.0419; 211.0396; 117.0344; 151.0033
34	18.87	isodaphnoretin B	C ₂₀ H ₁₄ O ₈	417.0404	[M-H] ⁻	5.2	151.0033
35	20.22	4',5-dihydroxy-3',7-dimethoxyflavone	C ₁₇ H ₁₄ O ₆	313.0722	[M-H] ⁻	1.4	255.0173; 190.9265; 138.9457

Table 1. Cont.

No.	Retention Time, T_R (min)	Compound Name	Molecular Formula	Detected Mass (m/z)	Ion Type	Mass Error (ppm)	MS/MS (m/z)
36	24.33	luteolin-3',4',7-trimethyl ether	C ₁₈ H ₁₆ O ₆	327.0869	[M-H] ⁻	-1.6	253.0563
37	25.08	syringaresinol	C ₂₂ H ₂₆ O ₈	463.1608	[M-H] ⁻	-0.4	121.0295
38	25.33	genkwanines O	C ₂₇ H ₃₆ O ₉	503.2287	[M-H] ⁻	0.1	315.16256; 239.09879; 194.08435; 121.03045
39	25.53	orthobenzoate 2	C ₂₇ H ₃₄ O ₈	485.2180	[M-H] ⁻	-0.3	297.1482; 121.0289
40	25.55	yuanhuapin	C ₂₉ H ₃₄ O ₁₀	541.2082	[M-H] ⁻	0.5	293.1180; 121.0292
41	26.98	(4S,5R,7S)-4,11-dihydroxy-guaia-1(2),9(10)-dien	C ₁₅ H ₂₄ O ₂	235.1703	[M-H] ⁻	-0.4	183.1391
42	27.11	genkwanoids H	C ₁₅ H ₂₂ O ₄	265.1481	[M-H] ⁻	13.4	251.1976; 116.9276
43	27.52	daphgenkin F	C ₃₁ H ₃₆ O ₁₀	567.2239	[M-H] ⁻	0.6	183.0126
44	28.10	(3 β ,12 α ,13 α)-3,12-dihydroxypimara-7,15-dien-2-one	C ₂₀ H ₃₀ O ₃	363.2151	[M-H] ⁻	-7.2	277.2172; 195.1391
45	28.3	genkwadaphnin	C ₃₄ H ₃₄ O ₁₀	601.2074	[M-H] ⁻	-0.9	309.1132; 187.0764; 121.0292
46	28.58	yuanhuatin	C ₃₄ H ₃₆ O ₁₀	603.2230	[M-H] ⁻	-1	121.0292; 253.1231
47	28.63	12-hydroxdaphnetoxin	C ₃₄ H ₃₆ O ₁₀	543.2604	[M-H] ⁻	0.8	167.1078
48	29.15	daphgenkin B	C ₃₇ H ₄₈ O ₁₂	683.3051	[M-H] ⁻	-3.2	309.1728; 183.0119; 471.3462
49	29.45	genkwanines D	C ₃₄ H ₄₀ O ₁₀	607.2551	[M-H] ⁻	0.4	327.1242; 309.1743; 187.0754; 165.0921; 121.0297
50	29.47	yuanhuagine	C ₃₄ H ₄₀ O ₁₀	583.2553	[M-H] ⁻	0.7	327.1242; 311.1690; 165.0921; 121.0297
51	30.12	genkwanines M	C ₃₄ H ₃₈ O ₉	589.2442	[M-H] ⁻	-0.3	467.2066; 121.0295
52	30.21	yuanhuadine/isoyuanhuadine	C ₃₂ H ₄₂ O ₁₀	585.2703	[M-H] ⁻	-0.4	281.1181; 167.1078; 123.1175
53	30.64	excoecariatoxin	C ₃₂ H ₄₂ O ₁₀	527.2647	[M-H] ⁻	-0.7	167.1068
54	30.83	12-O-N-deca-2,4,6-trienoyl-phorbol-(13)-acetate	C ₃₂ H ₄₂ O ₈	599.2858	[M-H] ⁻	-0.7	309.1117; 167.1073
55	31.22	yuanhuajine	C ₃₇ H ₄₂ O ₁₀	645.2699	[M-H] ⁻	0.5	277.2140; 225.2216; 165.0934
56	31.44	genkwadane D	C ₃₄ H ₄₆ O ₁₀	613.3010	[M-H] ⁻	-0.3	295.1881; 167.1075
57	31.76	genkwanines C	C ₃₇ H ₄₈ O ₁₀	651.3160	[M-H] ⁻	-2.3	293.1792; 165.0922
58 *	31.84	yuanhuacine	C ₃₇ H ₄₄ O ₁₀	647.2853	[M-H] ⁻	-1.3	327.1231; 309.1131; 281.1182; 167.1077; 121.0294
59	31.87	genkwanine F	C ₃₇ H ₅₀ O ₁₀	699.3366	[M-H+HCOOH] ⁻	-2.9	299.0557
60	31.98	daphgenkin A	C ₃₇ H ₄₆ O ₁₁	279.2331	[M-H] ⁻	0.4	183.0124; 116.9284
61	32.18	linoleic acid	C ₁₈ H ₃₂ O ₂	279.2331	[M-H] ⁻	0.4	183.0115; 116.9274
62	32.31	neogenkwanineE/neogenkwanineF	C ₃₇ H ₅₀ O ₁₀	653.3326	[M-H] ⁻	-0.8	167.1072; 121.0297
63	32.43	acutilonine F	C ₃₇ H ₄₆ O ₉	633.3064	[M-H] ⁻	-0.8	467.2066; 325.1841; 165.0921
64	32.94	wikstroemia factor M1	C ₃₇ H ₄₆ O ₁₀	635.3226	[M-H] ⁻	0.1	167.1067
65	33.05	palmitic acid	C ₁₆ H ₃₂ O ₂	255.2333	[M-H] ⁻	1.4	183.0124; 116.9287
66	33.29	oleic acid	C ₁₈ H ₃₄ O ₂	281.2488	[M-H] ⁻	0.7	183.0121
67	37.11	eleutheroside A	C ₃₅ H ₆₀ O ₆	621.4369	[M-H] ⁻	-0.5	183.0114; 130.9430

* Identified using reference standards.

2.2.1. Identification of Flavonoids

DG contains various flavonoids that can be classified into several types, including flavones, flavonols, and flavonoid glycosides. The fragmentation behaviors, such as retro-Diels–Alder (RDA) fragmentation and loss of neutral fragments, were mainly observed in the C- and A-rings and resulted in the production of numerous complex mass fragments.

The fragmentation patterns of genkwanin, hydroxygenkwanin, and luteolin-7-O- β -D-glucuronide were selected as representative examples of the three types of flavonoids. The flavone genkwanin produced a comparatively high response in the negative ion mode. Genkwanin showed the presence of a quasi-molecular ion of $[M-H]^-$ at m/z 283.0593, detected at a retention time of 18.81 min, along with an extremely strong base peak corresponding to $(C_{15}H_8O_5\bullet^-)$ at m/z 268.0356 with a loss of CH_3 (15 Da). Other minor product ions were detected at m/z 240.0419 ($C_{14}H_8O_4\bullet^-$), 211.0396 ($C_{13}H_7O_3\bullet^-$), 117.0344 ($C_8H_5O^-$), and 151.0033 ($C_7H_3O_4\bullet^-$), with successive losses of CO (28 Da) and CHO (29 Da) and RDA cleavage. Hydroxygenkwanin is a flavonol, and the fragmentation pattern showed the peak of a quasi-molecular $[M-H]^-$ ion at m/z 299.0553 and 13.82 min. Fragment peaks at m/z 284.0338 ($C_{15}H_8O_6\bullet^-$), 256.0389 ($C_{14}H_8O_5\bullet^-$), 227.0343 ($C_{13}H_7O_4\bullet^-$), 151.0039 ($C_7H_3O_4\bullet^-$), and 133.0309 ($C_8H_5O_2^-$) were detected in the MS2 spectrum with the loss of CH_3 , CO, and CHO and RDA cleavage in the C-ring.

The fragmentation pattern of luteolin-7-O- β -D-glucuronide, a typical flavonoid glycoside with a glucoside substituent, showed the presence of an $[M-H]^-$ molecular ion at m/z 461.0680 and 5.23 min, exhibiting relatively high numbers of MS2 fragments detected at m/z 285.0434 ($C_{15}H_9O_6^-$), 151.0036 ($C_7H_3O_4^-$), and 133.0296 ($C_8H_5O_2^-$), among others. A comparison of these spectra with the MS2 spectrum of the standard and those in the published literature [32] identified the three compounds as genkwanin, hydroxygenkwanin, and luteolin-7-O- β -D-glucuronide. The proposed fragmentation patterns are shown in Figure 2A–C.

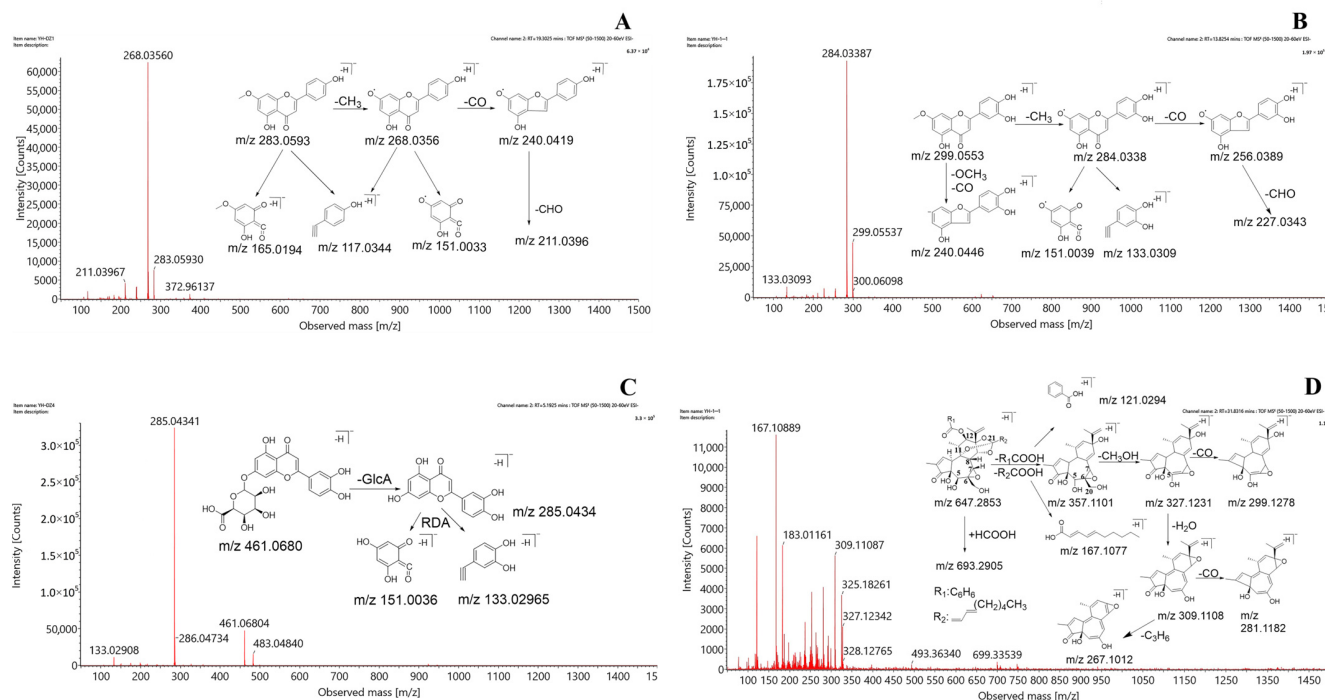


Figure 2. Cont.

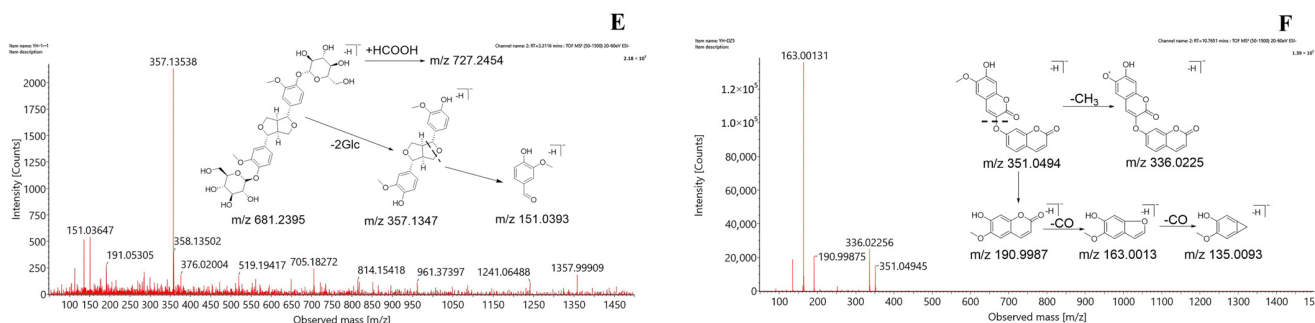


Figure 2. Mass spectra and proposed fragmentation pathways of (A) genkwanin, (B) hydroxy-genkwanin, (C) luteolin-7-O-β-D-glucuronide, (D) yuanhuacine, (E) pinores inoldiglucoside, and (F) daphnoretin.

2.2.2. Identification of Diterpene Esters

Daphnane-type diterpene esters are a class of important natural compounds with non-negligible toxicity [33]. Diterpene esters typically produce a series of predominant fragment ions originating from the successive or simultaneous loss of H₂O, CO, CH₃O, a chain of fatty acids and benzene groups, or a chain of fatty and benzoic acids. Yuanhuacine, which is found in DG, was selected as a representative daphnane-type diterpene ester to elucidate the fragmentation behavior and facilitate the structural characterization of other diterpenoids. With a molecular formula of C₃₇H₄₄O₁₀, the quasi-molecular [M-H]⁻ ion at *m/z* 647.2853 produced abundant fragment ions via the loss of H₂O, C₃H₆, CO, CH₃COOH, and C₇H₅O₂. First, the C12 substituents (R₁COOH) were eliminated via bond scission, followed by elimination via the bond scission of the C21 substituents (R₂COOH) to form the main fragment ion, [M-H-RCOOH]⁻, detected at *m/z* 357.1101. [M-H-RCOOH]⁻ is an important ion for inferring the structure of diterpenes and indicating the structure of the diterpenoid parent ring after the loss of the oxygen-substituted side chain. The substituents formed other fragment ions of C₇H₅O₂⁻ and C₁₀H₁₅O₂⁻ at *m/z* 121.0294 and 167.1077, respectively. Second, the epoxides at the C6 and C7 positions were prone to α-cleavage, resulting in the formation of the [M-H-CH₃OH•]⁻ and [M-H-CH₃OH-H₂O•]⁻ ions detected at *m/z* 327.1231 and 309.1108, respectively. These important ions indicated the substitution or lack of the hydroxyl groups at the C20 position. Finally, the fragment ion detected at *m/z* 327.1231 led to further successive or simultaneous losses of CO, H₂O, and C₃H₆, resulting in the product ions with peaks at *m/z* 299.1278, 281.1182, and 267.1012, respectively. The identification of yuanhuacine was validated using previous reports [34] and the MS₂ spectrum of the yuanhuacine standard solution. Figure 2D illustrates the probable fragmentation pathways of yuanhuacine. Subsequently, other daphnane-type diterpene esters were also identified and confirmed.

2.2.3. Identification of Lignan and Coumarin

In addition to flavonoids and diterpene esters, DG contained lignans and coumarins, which were obtained using traditional extraction and isolation techniques.

The representative lignan, pinores inoldiglucoside, readily forms [M-H]⁻ quasi-molecular ions in the negative ion mode and exhibits a common pattern of mass spectrometric cleavage: the quasi-molecular ion first loses 1–2 glucose molecules, after which the tetrahydrofuran ring opens with the loss of CH₃, CH₂O, CO, CH₃O, CH₃OH, and other groups, generating characteristic fragment ions above *m/z* 151. Figure 2E illustrates the possible fragmentation pathways of pinore inoldiglucoside. The identification process of lignin glycosides is briefly illustrated using the example of pinoresinol diglucoside, which forms an [M-H]⁻ excimer ion that is observed at *m/z* 681.2395 in the negative ion mode. The daughter ions, formed by the loss of two glucose molecules (162 Da) from the parent ion under the influence of collision voltage, were observed at *m/z* 519.1941 and 357.1353. The appearance of the characteristic fragment ion at *m/z* 151.0393 suggests that the compound

may be a lignin disaccharide compound. The combination of control experiments and literature reports [35] led to the identification of this compound and other lignans.

Dicoumarin daphnoretin was used as a reference standard to explore the cleavage pattern of coumarin under the aforementioned conditions. The dicoumarin daphnoretin molecule contains oxygen atoms and hydroxyl groups connected with aromatic rings and generally loses CH_3 and CO fragment ions in succession. Daphnoretin first fragments into monocoumarin, with an m/z of 190.9987. The fragment ion with m/z 190.9987 is then released from the middle of the double coumarin, followed by the loss of two molecules of CO, which yield the fragment ion peaks at m/z 163.0013 and 135.0093 [35]. The proposed fragmentation patterns are depicted in Figure 2F.

2.3. Multivariate Statistical Analysis

To identify the marker compounds that characterize the differences between CHDG and VPDG, the two sample groups were subjected to UPLC-Q-TOF-MS analysis, and the tandem mass spectrometry (MSE) raw data were processed for alignment, deconvolution, and data reduction using the Progenesis QI software (Waters, Milford, MA, USA) [36]. Progenesis QI detects chromatographic peaks to extract variables ($t\text{R}$, m/z , and intensity), normalizes, aligns similar variables, and creates a data matrix before presenting the results in a marker table. A Progenesis QI processing method was created, and the main parameters were as follows: retention time range, 0–38 min; minimum intensity, 5%; mass range, 50–1500 Da; mass tolerance, 0.10; mass window, 0.20; marker intensity threshold, 2000 counts; retention time window, 0.20; noise elimination level, 6. All processed data, including the m/z – $t\text{R}$ pairs from each data file and the corresponding intensities of all the detected peaks, were exported and analyzed using the SIMCA 14.1 software. In different batches of samples, components with the same $t\text{R}$ and m/z values were regarded as identical. Orthogonal projections to latent structures discriminant analysis (OPLS-DA) was performed to obtain the maximum separation between two different samples and explore the potential chemical markers responsible for the differences. In the sufficient permutation test, the R_{2Y} and Q₂ of the OPLS-DA model were 0.92 and 0.82, respectively, which indicated an acceptable validity for the subsequent identification of the characteristic markers (Figure 3A). S plots were then created to visualize the OPLS-DA predictive component loading to facilitate the interpretation of the model, in which each point represented an ion RT- m/z pair. The x-axis represented the variable contribution; ion RT- m/z pair points that are located further away from zero indicate a higher contribution of the ion to the difference between the two groups. The y-axis represented the variable confidence; ion RT- m/z pair points that are located further away from zero indicate a higher confidence level that the ion contributed to the difference between the two groups. Therefore, the RT- m/z pair points at the two ends of the “S” shape represent the components that are the most responsible for the difference between these two types of samples, which can be regarded as the components that most differentiate between CHDG and VPDG [28,37–40] (Figure 3B). To investigate whether data overfitting occurred in the OPLS-DA model, 200 iterations of the permutation test were performed using the SIMCA 14.1 software, in which R_{2Y} and Q₂ described the explanation level of the model in the y-axis direction and the forecasted level of the model, respectively. Based on the permutation test, the intercept of the R₂ regression curve was less than 0.4, and that of the Q₂ regression curve was less than 0, indicating that the model was not overfitted and that the modeling was successful [39,41,42] (Figure 3C,D).

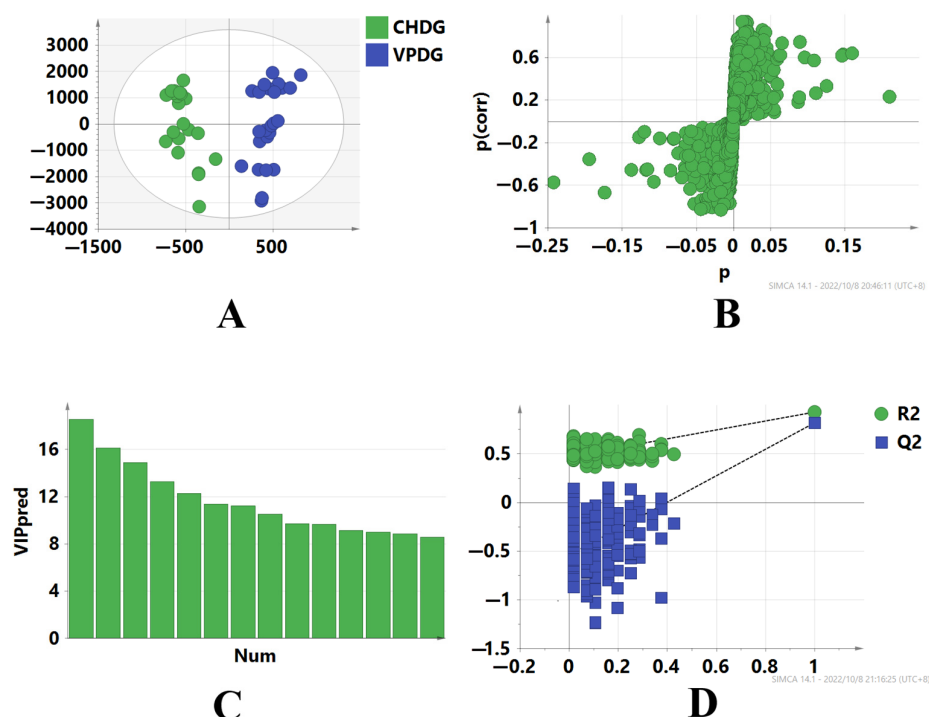


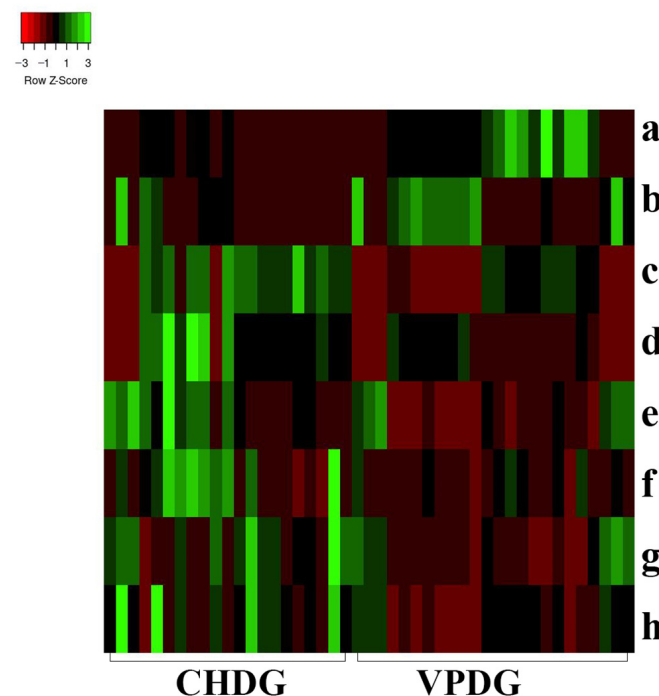
Figure 3. OPLS-DA scores plot and S-plot of CHDG and VPDG in the ESI[−] mode. (A) shows Hierarchical Clustering Alg (HCA) analysis results of CHDG and VPDG, (B) shows the S-plot of CHDG and VPDG, providing visualization of the OPLS–DA predictive component, (C) shows the Plot of Variable Importance for the Projection (VIP), which summarizes the importance of the variables, and (D) shows permutation tests of the model, which indicated that the predictive models were not overfitting.

2.4. Analysis of Chemicals of DG after Processing

In univariate statistical analysis, the multivariate statistical analysis condition, the variable importance for the projection (VIP) value, was set to >1. The *t*-test ($p < 0.05$) showed that 241 characteristic ions exhibited significant differences. Along with the component analysis, this test excluded the interference fragments and confirmed the molecular ions. A total of eight potential chemical markers were identified (Table 2). The mass accuracy of all assigned components was less than 5 ppm, relative to the empirical molecular formulas of the compounds known to exist in DG. To present the level of change in the differential compounds, a heat map was generated to show the relative levels of each compound in CHDG and VPDG [43] (Figure 4). The intensities of ions a and b were higher in VPDG than those in CHDG, indicating that the two components correlated to ions a and b could be used as potential characteristic markers to distinguish between VPDG and CHDG. Meanwhile, the intensities of ions c, d, e, f, g, and h were higher in CHDG than those in VPDG, indicating that the six components correlated to ions c–h may also be used as potential characteristic markers to distinguish CHDG from VPDG. The identities of the components a–g (Table 2) were further confirmed by comparing the mass/UV spectra and retention times with those of the reference compounds. Considering the identification of the most differentiating components between CHDG and VPDG, certain prominent ions were found to correspond to the deprotonated molecular ions of all components. The ions a–h correlated to compounds 15, 32, 38, 39, 26, 23, 6, and 28, respectively. The differentiating components 38 and 39 are well-known toxic components of DG; therefore, a reduction in their contents in VPDG suggests that stir-baking with vinegar could reduce the toxicity of CHDG.

Table 2. Identification of the most differentiating components between CHDG and VPDG.

Peak No.	RT (min)	HR-Mass (<i>m/z</i>)	Assigned Identity	VIP Value	<i>p</i> -Value
a	5.57	505.0988	apigenin-7-O-β-D-methylglucuronate	1.3322	0.0005
b	13.82	299.0562	hydroxygenkwanin	1.8095	0.0361
c	25.33	503.2287	genkwanines O	10.5276	0.0029
d	25.53	485.2180	orthobenzoate 2	18.576	8×10^{-5}
e	8.90	593.1298	tiliroside	14.9209	0.0173
f	6.28	301.0355	quercetin	3.6803	0.0074
g	3.37	179.0354	caffei acid	1.7246	0.0256
h	9.69	271.0611	naringenin	3.2516	0.0079

**Figure 4.** Heat map analysis of the potential biomarkers in both CHDG and VPDG. X-axis represents the different groups; y-axis represents the different metabolites. Metabolites represented by the letters a–h are presented in Table 2.

3. Experimental

3.1. Materials, Chemicals, and Reagents

Methanol (LC-MS grade) and acetonitrile (LC-MS grade) were purchased from Fisher (Pittsburgh, PA, USA). LC-MS grade formic acid was purchased from Merck Millipore (Darmstadt, Germany). Purified water was obtained using a Milli-Q purification system (Millipore, Bedford, MA, USA).

A total of 21 batches of CHDG were collected from different areas in China and authenticated by the authors. The corresponding voucher specimens were deposited in the Museum of Traditional Chinese Medicine Specimens, Institute for the Control of Traditional Chinese Medicine and Ethnic Medicine. A total of 24 batches of VPDG were prepared according to the standards of the Chinese Pharmacopoeia 2020. Details of the samples, including their source and batch number, are provided in Table 3.

Table 3. Detailed information on CHDG and VPDG samples.

Sample No.	Batch No.	Sample	Batch No.	Source
CHDG01-1	Self-collection-1	VPDG 01-2	/	Wugang, Henan province
	Self-collection-1	VPDG 01-3	/	
CHDG02-1	Self-collection-1	VPDG 02-2	/	Anhui province
		VPDG 02-3	/	
CHDG03-1	Self-collection-2	VPDG 03-2	/	Henan province
	Self-collection-3	VPDG 03-3	/	
CHDG04-1	Self-collection-4	VPDG 04-2	/	Anhui province
CHDG05-1	Self-collection-5	VPDG 05-2	/	Henan province
CHDG06-1	Self-collection-6	VPDG 06-2	/	Henan province
CHDG07-1	Self-collection-7	VPDG 07-2	/	Henan province
CHDG08-1	Self-collection-8	VPDG 08-2	/	Hubei province
CHDG09-1	Self-collection-9	VPDG 09-2	/	Hubei province
CHDG010-1	Self-collection-10	VPDG 010-2	/	Hubei province
CHDG011-1	Self-collection-11	VPDG 011-2	/	Hubei province
CHDG012-1	Self-collection-12	VPDG 012-2	/	Hubei province
CHDG013-1	H1901290	VPDG 013-2	H190129001-3	Luotian, Hunan province
CHDG014-1	H1901300	VPDG 014-2	H190130001-3	Zhangshu, Jiangxi province
CHDG015-1	H1901310	VPDG 015-2	H190131001-3	Deqing, Zhejiang province
CHDG016-1	H1901320	VPDG 016-2	H190132001-3	Dawu, Hubei province
CHDG017-1	H1901330	VPDG 017-2	H190133001-3	Jingzhai, Anhui province
CHDG018-1	H1901340	VPDG 018-2	H190134001-3	Xiaogan, Hubei province
CHDG019-1	H1901350	VPDG 019-2	H190135001-3	Nanyang, Henan province
CHDG020-1	H1901360	VPDG 020-2	H190136001-3	Dawu, Hubei province
CHDG021-1	H1901370	VPDG 021-2	H190137001-3	Zhengyang, Henan province
CHDG022-1	H1901380	VPDG 022-2	H190138001-3	Zaoyang, Hubei province

3.2. Sample Preparation and Extraction

All DG samples were air-dried, ground, and sieved (Chinese National Standard Sieve 4, 65-mesh) to obtain a homogeneous powder. Each powder was weighed (approximately 1.0 g) and mixed with 70% methanol (50 mL). Each sample was then extracted at 40 °C for 50 min in an ultrasonic bath (power, 240 W; frequency, 45 kHz). After cooling to 20 °C, weight loss was replenished with 70% methanol. The extraction solution was then filtered through a syringe filter (0.22 µm) and injected into the UPLC system.

3.3. Chromatography Separation

Chromatographic separation was performed on an ACQUITY UPLC HSS T3 C18 column (100 mm × 2.1 mm, 1.8 µm; Waters, USA) using an ACQUITY UPLC system (Waters Co., Milford, MA, USA). The mobile phase was composed of eluent A (0.1% formic acid in water, v/v) and eluent B (acetonitrile), with a flow rate of 0.3 mL/min. The optimized gradient elution program was as follows: 0→1.5 min, 8–18% B; 1.5→4 min, 18–23% B; 4→5 min, 23–40% B; 5→20 min, 40–40% B; 20→32 min, 40–95% B; 32→37 min, 95% B; 37→38 min, 95–8% B; 38→45 min, 8% B. The temperatures of the autosampler and UPLC column manager were set at 10 and 35 °C, respectively. The injection volume was 0.5 µL.

3.4. Mass Spectrometry

UPLC-Q-TOF-MS was performed using a Waters SYNAPT G2-S QTOF mass spectrometer (Waters Co., Milford, MA, USA), with Q-TOF technology, UPLC fast DDA, and a UPLC/MSE instrument equipped with a UPLC system through an ESI interface to achieve high levels of sensitivity, selectivity, speed, and accuracy. The mass spectrum was acquired from 50 to 1500 Da in the MSE mode with a scan time of 0.2 s and detection time of 37 min. The negative ion mode conditions were as follows: capillary voltage, 2.5 kV; source temperature, 120 °C; desolvation temperature, 350 °C; cone voltage, 40 V; cone gas flow rate, 50 L/h; desolvation gas flow rate, 600 L/h. In the MSE mode, data acquisition was performed via the mass spectrometer by rapidly switching from a low collision energy (CE) scan to a high CE scan during a single LC analysis. The low energy function was set to 6 V, and the ramp CE of the high energy function was set to 20–60 eV. Leucine enkephalin (LE, 0.2 pg/mL, *m/z* 554.2620 in the ESI[−] mode), the external reference of Lock Spray, was infused at a constant flow rate of 10 µL/min and monitored in the negative ion

mode. During acquisition, data were collected in the continuum mode for screening and multivariate statistical analyses.

3.5. Mass Data Processing and Analysis

The raw data were precaptured and processed using the Waters MassLynx V4.2 software. The data were analyzed using the UNIFI and Progenesis QI software, in combination with a self-built compound library and a fragment ion matching strategy, to fully characterize the chemical composition of DG. The main data processing parameters included the retention time, molecular *m/z*, and mass error range, whereas secondary fragment ion information was used to infer the compound structure. Before identifying the compounds, a comprehensive library of the chemical composition of DG was created by systematically searching CNKI, PubChem, ChemicalBook, and other databases [3,44]. This in-house database includes the names of compounds, molecular formulas, molecular weights, chemical structural formulas, molecular ions, and secondary fragment ions. The chemical components were identified using the UNIFI software. Ion peaks with retention times within 0.2 min and an *m/z* within 10 ppm of each other were identified as those of the same compound.

4. Conclusions

DG is a toxic herb used in TCM that requires stir-baking with vinegar to reduce its toxicity prior to oral administration. Studies on HL-7702 cells have shown that vinegar treatment reduces hepatotoxicity induced by DG [45]. However, the potential mechanisms underlying this reduction in hepatotoxicity require further investigation. Our previous research has shown that methanol extracts contain the main hepatotoxic components of DG, particularly diterpene esters [46,47]; therefore, the methanol fraction of DG was selected as the target in this study.

Screening analysis using UPLC-Q-TOF-MS identified a total of 67 compounds from the buds of DG. The quantity and strength of the responses of the identified compounds in the TIC chromatograms indicated that the performance of the negative ionization mode was superior to that of the positive ionization mode. The 67 identified compounds, including flavones, flavonols, flavonoid glycosides, daphnane-type diterpene esters, lignans, and coumarins, were constituents of both CHDG and VPDG, which implied that they were similar in terms of their composition. Eight compounds in the methanol extracts were identified as major contributors to the differences between CHDG and VPDG: apigenin-7-O- β -D-methylglucuronate (a), hydroxygenkwanin (b), genkwanines O (c), orthobenzoate 2 (d), tiliroside (e), quercetin (f), caffeic acid (g), and naringenin (h). Considering their toxicity [48–51], the reduction in the amount of daphnane-type diterpene ester compounds in VPDG might explain the mechanism through which stir-baking with vinegar reduces the toxicity of CHDG. In addition to the aforementioned compounds, other compounds not listed here contributed to the differences between CHDG and VPDG. Future studies should involve controlling the levels of apigenin-7-O- β -D-methylglucuronate (a) and hydroxygenkwanin (b) to ensure the quality of VPDG, as well as controlling the levels of genkwanines O (c), orthobenzoate 2 (d), tiliroside (e), quercetin (f), caffeic acid (g), and naringenin (h) in CHDG to establish a method for ensuring the quality of this traditional medicine. Furthermore, future studies will focus on establishing standards to ensure the quality of both CHDG and VPDG and examining the ways in which changes in the level of internal chemical compounds affect the pharmacological effects. Future studies should also involve the study of the connotation and mechanism of TCM processing technology.

In this study, we established an efficient method that employs UPLC-Q-TOF-MS coupled with chemometrics to differentiate between and detect CHDG and VPDG by identifying potential chemical markers. This approach enabled the detailed profiling of each sample such that numerous chemical markers could be detected and used as powerful indices to identify and distinguish between CHDG and VPDG. The present approach provides a foundation for the detection of ion pairs derived from the parent ion and

a fragment ion of the chemical markers using the MRM mode of LC/MS/MS and for developing a sensitive, stable, and rapid quality control standard for Chinese medicinal materials and relevant processed decoction pieces.

Author Contributions: H.M. and P.Z. performed the experiments and wrote the paper. L.Y. collected the test samples, and F.W. acquired and analyzed the data. S.M. interpreted the data. P.Z. and H.G. conceived and designed the study, and T.L. provided guidance for the implementation of the experimental scheme. All authors have read and agreed to the published version of the manuscript.

Funding: This work was partly supported by grants from the project “The Quality Standard and Scientific Control Research of Toxic Chinese Herbal Decoction Pieces” (Grant No. 2018YFC1707003) of the Important Program of the Ministry of Science and Technology of the People’s Republic of China.

Institutional Review Board Statement: The study did not require ethical approval.

Informed Consent Statement: The study did not involve humans.

Data Availability Statement: We stated that the research data was analyzed based on commercial data analysis software, there is no publicly archived datasets or generated new datasets. We will accumulate data in the next work and gradually generate available datasets.

Acknowledgments: We sincerely thank engineers Chao Zhou and technical experts Jing Wang from Waters Technology Co., Ltd., (Shanghai, China) and Zhijie Zhang from the Institute of Chinese Materia Medica, Chinese Academy of Chinese Medical Sciences, for their expert technical assistance.

Conflicts of Interest: The authors declare no conflict of interest. Funding sponsors had no role in the design of the study; in the collection, analyses, or interpretation of data; in the writing of the manuscript; or in the decision to publish results.

Sample Availability: Samples of the compounds of apigenin-7-O- β -D-methylglucuronate, hydroxygenkwanin, tiliroside, quercetin, and caffeic acid are available from the authors.

References

- Wu, X.; Wang, S.P.; Lu, J.R.; Jing, Y.; Li, M.X.; Cao, J.L.; Bian, B.L.; Hu, C.J. Seeing the unseen of Chinese herbal medicine processing (Paozhi): Advances in new perspectives. *Chin. Med.* **2018**, *13*, 4. [[CrossRef](#)] [[PubMed](#)]
- Ota, M.; Nagachi, Y.; Ishiuchi, K.; Tabuchi, Y.; Xu, F.; Shang, M.Y.; Cai, S.Q.; Makino, T. Comparison of the inducible effects of licorice products with or without heat-processing and pre-treatment with honey on granulocyte colony-stimulating factor secretion in cultured enterocytes. *J. Ethnopharmacol.* **2018**, *214*, 1–7. [[CrossRef](#)] [[PubMed](#)]
- Wang, M.; Fu, J.F.; Lv, M.Y.; Tian, Y.; Xu, F.G.; Song, R.; Zhang, Z.J. Effect of wine processing and acute blood stasis on the serum pharmacocochemistry of rhubarb: A possible explanation for processing mechanism. *J. Sep. Sci.* **2014**, *37*, 2499–2503. [[CrossRef](#)]
- Wu, L.Y.; Yang, Y.; Mao, Z.J.; Wu, J.J.; Ren, D.; Zhu, B.; Qin, L.P. Processing and Compatibility of Corydalis yanhusuo: Phytochemistry, Pharmacology, Pharmacokinetics, and Safety. *Evid. Based Complement. Altern. Med.* **2021**, *2021*, 1271953. [[CrossRef](#)] [[PubMed](#)]
- Zhang, L.; Guo, W.F.; Liang, H.; Zhu, X.H.; Na, B.Q.; Xu, J.F.; Zhang, C.H.; Li, M.H. Study on traditional processing method of Mongolian medicine and excipient usage based on data mining. *Zhongguo Zhong Yao Za Zhi* **2020**, *45*, 3988–3996. [[PubMed](#)]
- Cai, B.C.; Qin, K.M.; Wu, H.; Cai, H.; Lu, T.L.; Zhang, X.D. Chemical mechanism during Chinese medicine processing. *Prog. Chem.* **2012**, *24*, 637–649. [[CrossRef](#)]
- Yu, J.G.; Guo, J.; Zhu, K.Y.; Tao, W.; Chen, Y.; Liu, P.; Hua, Y.; Tang, Y.; Duan, J.A. How impaired efficacy happened between Gancao and Yuanhua: Compounds, targets and pathways. *Sci. Rep.* **2017**, *7*, 3828. [[CrossRef](#)]
- Hong, J.Y.; Chung, H.J.; Lee, H.J.; Park, H.J.; Lee, S.K. Growth inhibition of human lung cancer cells via down-regulation of epidermal growth factor receptor signaling by yuanhuadine, a daphnane diterpene from *Daphne genkwa*. *J. Nat. Prod.* **2011**, *74*, 2102–2108. [[CrossRef](#)]
- Li, S.M.; Chou, G.X.; Hseu, Y.C.; Yang, H.L.; Kwan, H.Y.; Yu, Z.L. Isolation of anticancer constituents from flos genkwa (*Daphne genkwa* Sieb. et Zucc.) through bioassay-guided procedures. *Chem. Cent. J.* **2013**, *7*, 159. [[CrossRef](#)]
- Yoo, N.; Lee, H.R.; Son, J.M.; Kang, H.B.; Lee, H.G.; Yoon, S.R.; Yoon, S.Y.; Kim, J.W. Genkwadaphnin promotes leukocyte migration by increasing CD44 expression via PKD1/NF- κ B signaling pathway. *Immunol. Lett.* **2016**, *173*, 69–76. [[CrossRef](#)]
- Bailly, C. Yuanhuacin and related anti-inflammatory and anticancer daphnane diterpenes from Genkwa Flos—An overview. *Biomolecules* **2022**, *12*, 192. [[CrossRef](#)] [[PubMed](#)]
- Lee, M.Y.; Park, B.Y.; Kwon, O.K.; Yuk, J.E.; Oh, S.R.; Kim, H.S.; Lee, H.K.; Ahn, K.S. Anti-inflammatory activity of (-)-aptosimon isolated from *Daphne genkwa* in RAW264.7 cells. *Int. Immunopharmacol.* **2009**, *9*, 878–885. [[CrossRef](#)]

13. Li, Y.N.; Yin, L.H.; Xu, L.N.; Peng, J.Y. A simple and efficient protocol for large-scale preparation of three flavonoids from the flower of *Daphne genkwa* by combination of macroporous resin and counter-current chromatography. *J. Sep. Sci.* **2010**, *33*, 2168–2175. [CrossRef] [PubMed]
14. Xie, H.; Liang, Y.; Ito, Y.; Wang, X.; Chen, R.; He, J.; Li, H.; Zhang, T. Preparative isolation and purification of four flavonoids from *Daphne genkwa* Sieb. et Zucc. by high-speed countercurrent chromatography. *J. Liq. Chromatogr. Relat. Technol.* **2011**, *34*, 2360–2372. [CrossRef]
15. Mi, S.H.; Zhao, P.; Li, Q.; Zhang, H.; Guo, R.; Liu, Y.Y.; Lin, B.; Yao, G.D.; Song, S.J.; Huang, X.X. Guided isolation of daphnane-type diterpenes from *Daphne genkwa* by molecular network strategies. *Phytochemistry* **2022**, *198*, 113144. [CrossRef]
16. Pan, R.R.; Zhang, C.Y.; Li, Y.; Zhang, B.B.; Zhao, L.; Ye, Y.; Song, Y.N.; Zhang, M.; Tie, H.Y.; Zhang, H.; et al. Daphnane Diterpenoids from *Daphne genkwa* inhibit PI3K/Akt/mTOR signaling and induce cell cycle arrest and apoptosis in human colon cancer cells. *J. Nat. Prod.* **2020**, *83*, 1238–1248. [CrossRef] [PubMed]
17. Zhan, Z.J.; Fan, C.Q.; Ding, J.; Yue, J.M. Novel diterpenoids with potent inhibitory activity against endothelium cell HMEC and cytotoxic activities from a well-known TCM plant *Daphne genkwa*. *Bioorg. Med. Chem.* **2005**, *13*, 645–655. [CrossRef] [PubMed]
18. Park, B.Y.; Min, B.S.; Oh, S.R.; Kim, J.H.; Bae, K.H.; Lee, H.K. Isolation of flavonoids, a biscoumarin and an amide from the flower buds of *Daphne genkwa* and the evaluation of their anti-complement activity. *Phytother. Res.* **2006**, *20*, 610–613. [CrossRef] [PubMed]
19. Zhang, C.Y.; Luo, L.; Xia, J.; Song, Y.N.; Zhang, L.J.; Zhang, M.; Rahman, K.; Ye, Y.; Zhang, H.; Zhu, J.Y. Sesquiterpenes and lignans from the flower buds of *Daphne genkwa* and their nitric oxide inhibitory activities. *Nat. Prod. Res.* **2018**, *32*, 2893–2899. [CrossRef]
20. Gan, L.; Ji, J.; Wang, L.; Li, Q.Y.; Zhang, C.F.; Wang, C.Z.; Yuan, C.S. Identification of the metabolites in normal and AA rat plasma, urine and feces after oral administration of *Daphne genkwa* flavonoids by LC-Q-TOF-MS spectrometry. *J. Pharm. Biomed. Anal.* **2020**, *177*, 112856. [CrossRef]
21. Zhao, H.D.; Lu, Y.; Yan, M.; Chen, C.H.; Morris-Natschke, S.L.; Lee, K.H.; Chen, D.F. Rapid recognition and targeted isolation of anti-HIV daphnane diterpenes from *Daphne genkwa* guided by UPLC-MS(n). *J. Nat. Prod.* **2020**, *83*, 134–141. [CrossRef] [PubMed]
22. Du, W.J.; Ji, J.; Wang, L.; Lan, X.Y.; Li, J.; Lei, J.Q.; He, X.; Zhang, C.F.; Huang, W.Z.; Wang, Z.Z.; et al. Relationship between the UPLC-Q-TOF-MS fingerprinted constituents from *Daphne genkwa* and their anti-inflammatory, anti-oxidant activities. *Biomed. Chromatogr.* **2017**, *31*, e4012. [CrossRef] [PubMed]
23. Yuan, S.; Wang, Z.; Xia, K. Comprehensive evaluation and practical confirmation on processing technology of *Daphne genkwa* Sieb. et Zucc. *Zhongguo Zhong Yao Za Zhi* **1999**, *24*, 464–465, 510. [PubMed]
24. Zhang, C.F.; Zhang, S.L.; He, X.; Yang, X.L.; Wu, H.T.; Lin, B.Q.; Jiang, C.P.; Wang, J.; Yu, C.H.; Yang, Z.L.; et al. Antioxidant effects of Genkwa Flos flavonoids on Freund's adjuvant-induced rheumatoid arthritis in rats. *J. Ethnopharmacol.* **2014**, *153*, 793–800. [CrossRef]
25. Zhou, D.C.; Zheng, G.; Jia, L.Y.; He, X.; Zhang, C.F.; Wang, C.Z.; Yuan, C.S. Comprehensive evaluation on anti-inflammatory and anti-angiogenic activities in vitro of fourteen flavonoids from *Daphne genkwa* based on the combination of efficacy coefficient method and principal component analysis. *J. Ethnopharmacol.* **2021**, *268*, 113683. [CrossRef]
26. Zhou, Q.R.; Xiao, L.Y.; Liu, Q.N.; Sun, P.P.; Zhang, L. Vinegar processing attenuates toxicity on IEC-6 cells caused by chloroform extraction of *Daphne genkwa*. *Zhongguo Zhong Yao Za Zhi* **2018**, *43*, 2282–2287.
27. Chen, Y.; Guo, J.; Tang, Y.; Wu, L.; Tao, W.; Qian, Y.; Duan, J.A. Pharmacokinetic profile and metabolite identification of yuanhuapine, a bioactive component in *Daphne genkwa* by ultra-high performance liquid chromatography coupled with tandem mass spectrometry. *J. Pharm. Biomed. Anal.* **2015**, *112*, 60–69. [CrossRef]
28. Tao, Y.; Su, D.D.; Li, W.D.; Cai, B.C. Pharmacokinetic comparisons of six components from raw and vinegar-processed *Daphne genkwa* aqueous extracts following oral administration in rats by employing UHPLC-MS/MS approaches. *J. Chromatogr. B. Anal. Technol. Biomed. Life Sci.* **2018**, *1079*, 34–40. [CrossRef]
29. Gao, Y.; Wu, Y.; Liu, S.; Liu, Z.Q.; Song, F.R.; Liu, Z.Y. A strategy to comprehensively and quickly identify the chemical constituents in Platycodi Radix by ultra-performance liquid chromatography coupled with traveling wave ion mobility quadrupole time-of-flight mass spectrometry. *J. Sep. Sci.* **2021**, *44*, 691–708. [CrossRef]
30. Tian, P.P.; Zhang, X.X.; Wang, H.P.; Li, P.L.; Liu, Y.X.; Li, S.J. Rapid analysis of components in *Coptis chinensis* Franch by ultra-performance liquid chromatography with quadrupole time-of-flight mass spectrometry. *Pharmacogn. Mag.* **2017**, *13*, 175–179.
31. Oh, J.H.; Ha, I.J.; Lee, M.Y.; Kim, E.O.; Park, D.; Lee, J.H.; Lee, S.G.; Kim, D.W.; Lee, T.H.; Lee, E.J.; et al. Identification and metabolite profiling of alkaloids in aerial parts of *Papaver rheas* by liquid chromatography coupled with quadrupole time-of-flight tandem mass spectrometry. *J. Sep. Sci.* **2018**, *41*, 2517–2527. [CrossRef] [PubMed]
32. Yin, R.; Han, F.; Tang, Z.; Liu, R.; Zhao, X.; Chen, X.H.; Bi, K.S. UFLC-MS/MS method for simultaneous determination of luteolin-7-O-gentibioside, luteolin-7-O- β -D-glucoside and luteolin-7-O- β -D-glucuronide in beagle dog plasma and its application to a pharmacokinetic study after administration of traditional Chinese medicinal preparation: Kudiezi injection. *J. Pharm. Biomed. Anal.* **2013**, *72*, 127–133. [PubMed]
33. Park, B.Y.; Min, B.S.; Ahn, K.S.; Kwon, O.K.; Joung, H.; Bae, K.H.; Lee, H.K.; Oh, S.R. Daphnane diterpene esters isolated from flower buds of *Daphne genkwa* induce apoptosis in human myelocytic HL-60 cells and suppress tumor growth in Lewis lung carcinoma (LLC)-inoculated mouse model. *J. Ethnopharmacol.* **2007**, *111*, 496–503. [CrossRef] [PubMed]

34. Geng, L.L.; Sun, H.Y.; Yuan, Y.; Liu, Z.Z.; Cui, Y.; Bi, K.S.; Chen, X.H. Discrimination of raw and vinegar-processed Genkwa Flos using metabolomics coupled with multivariate data analysis: A discrimination study with metabolomics coupled with PCA. *Fitoterapia* **2013**, *84*, 286–294. [[CrossRef](#)]
35. Li, W.; Yang, M.H.; Zheng, Y.G. Fragmentation investigation of seven arylnaphthalide lignans using liquid chromatography/tandem quadrupole time-of-flight mass spectrometry. *Rapid Commun. Mass. Spectrom.* **2012**, *26*, 950–956. [[CrossRef](#)]
36. Zhang, J.X.; Yang, W.Z.; Li, S.R.; Yao, S.; Qi, P.; Yang, Z.; Feng, Z.J.; Hou, J.J.; Cai, L.Y.; Yang, M.; et al. An intelligentized strategy for endogenous small molecules characterization and quality evaluation of earthworm from two geographic origins by ultra-high performance HILIC/QTOF MS(E) and Progenesis QI. *Anal. Bioanal. Chem.* **2016**, *408*, 3881–3890. [[CrossRef](#)]
37. Huang, B.M.; Zha, Q.L.; Chen, T.B.; Xiao, S.Y.; Xie, Y.; Luo, P.; Wang, Y.P.; Liu, L.; Zhou, H. Discovery of markers for discriminating the age of cultivated ginseng by using UHPLC-QTOF/MS coupled with OPLS-DA. *Phytomedicine* **2018**, *45*, 8–17. [[CrossRef](#)]
38. Qi, S.; Zha, L.Y.; Peng, Y.Z.; Luo, W.; Chen, K.L.; Li, X.; Huang, D.F.; Yin, D.M. Quality and Metabolomics Analysis of *Houttuynia cordata* Based on HS-SPME/GC-MS. *Molecules* **2022**, *27*, 3921. [[CrossRef](#)]
39. Song, H.H.; Kim, D.Y.; Woo, S.; Lee, H.K.; Oh, S.R. An approach for simultaneous determination for geographical origins of Korean *Panax ginseng* by UPLC-QTOF/MS coupled with OPLS-DA models. *J. Ginseng Res.* **2013**, *37*, 341–348. [[CrossRef](#)]
40. Zeng, F.Q.; Xu, Y.L.; Li, Y.L.; Yan, Z.G.; Li, L. Metabonomics Study of the hematopoietic effect of medicinal wine Maoji Jiu on a blood deficiency rat model by ultra-high-performance liquid chromatography coupled to quadrupole time-of-flight mass spectrometry and a pattern recognition approach. *Molecules* **2022**, *27*, 3791. [[CrossRef](#)]
41. Wheelock, Å.M.; Wheelock, C.E. Trials and tribulations of ‘omics data analysis: Assessing quality of SIMCA-based multivariate models using examples from pulmonary medicine. *Mol. Biosyst.* **2013**, *9*, 2589–2596. [[CrossRef](#)] [[PubMed](#)]
42. Xu, Z.W.; Sheng, Y.X.; Zeng, G.W.; Zeng, Z.J.; Li, B.T.; Jiang, L.; Xu, G.L.; Zhang, Q.Y. Metabonomic study on the plasma of high-fat diet-induced dyslipidemia rats treated with Ge Gen Qin Lian decoction by ultrahigh-performance liquid chromatography-mass spectrometry. *Evid. Based Complement. Altern. Med.* **2021**, *2021*, 6692456. [[CrossRef](#)]
43. Nthai, D.; Thibane, V.S.; Gololo, S.S. Comparative study of abiotic stress factors on GC-MS-detected phytoconstituents of *Aloe greataeadii var: Davyana* using heat map and hierarchical clustering dendrogram. *Biochem. Res. Int.* **2022**, *2022*, 5365024. [[CrossRef](#)] [[PubMed](#)]
44. Gu, R.H.; Rybalov, L.; Negrin, A.; Morcol, T.; Long, W.W.; Myers, A.K.; Isaac, G.; Yuk, J.; Kennelly, E.J.; Long, C.L. Metabolic profiling of different parts of *Acer truncatum* from the Mongolian plateau using UPLC-QTOF-MS with comparative bioactivity assays. *J. Agric. Food Chem.* **2019**, *67*, 1585–1597. [[CrossRef](#)] [[PubMed](#)]
45. Geng, L.L. Metabonomic Study of Genkwa Flos-Induced Hepatic Injury and Detoxification of Herb-Processing. Ph.D. Dissertation, Shenyang Pharmaceutical University, Shenyang, China, 2013.
46. Campos, A.; Vendramini-Costa, D.B.; Longato, G.B.; Zermiani, T.; Ruiz, A.L.; de Carvalho, J.E.; Pandiella, A.; Cechinel Filho, V. Antiproliferative effect of *Synadenium grantii* Hook f. stems (Euphorbiaceae) and a rare phorbol diterpene ester. *Int. J. Toxicol.* **2016**, *35*, 666–671. [[CrossRef](#)] [[PubMed](#)]
47. Zayed, S.M.; Farghaly, M.; Soliman, S.M.; Gotta, H.; Sorg, B.; Hecker, E. Dietary cancer risk from conditional cancerogens (tumor promoters) in produce of livestock fed on species of spurge (Euphorbiaceae). V. Skin irritant and tumor-promoting diterpene ester toxins of the tigliane and ingenane type in the herbs *Euphorbia nubica* and *Euphorbia helioscopia* contaminating fodder of livestock. *J. Cancer Res. Clin. Oncol.* **2001**, *127*, 40–47. [[PubMed](#)]
48. Ma, X.H.; Wang, Z.B.; Zhang, L.; Li, W.; Deng, C.M.; Zhong, T.H.; Li, G.Y.; Zheng, W.M.; Zhang, Y.H. Diterpenoids from *Wedelia prostrata* and their derivatives and cytotoxic activities. *Chem. Biodivers.* **2017**, *14*, e1600423. [[CrossRef](#)]
49. Samadder, A.; Das, J.; Das, S.; Das, D.; De, A.; Bhadra, K.; Khuda-Bukhsh, A.R. Dihydroxy-isosteviol methyl ester of *Pulsatilla nigricans* extract reduces arsenic-induced DNA damage in testis cells of male mice: Its toxicity, drug-DNA interaction and signaling cascades. *Zhong Xi Yi Jie He Xue Bao* **2012**, *10*, 1433–1442. [[CrossRef](#)]
50. Zayed, S.M.; Farghaly, M.; Taha, H.; Gminski, R.; Hecker, E. Dietary cancer risk from conditional cancerogens in produce of livestock fed on species of spurge (Euphorbiaceae). III. Milk of lactating goats fed on the skin irritant herb *Euphorbia peplus* is polluted by tumor promoters of the ingenane diterpene ester type. *J. Cancer Res. Clin. Oncol.* **1998**, *124*, 301–306.
51. Zhou, S.K.; Zhang, Y.; Ju, Y.H.; Zhang, Q.; Luo, D.; Cao, Y.D.; Yao, W.F.; Tang, Y.P.; Zhang, L. Comparison of content-toxicity-activity of six ingenane-type diterpenoids between *Euphorbia kansui* before and after stir-fried with vinegar by using UFLC-MS/MS, zebrafish embryos and HT-29 cells. *J. Pharm. Biomed. Anal.* **2021**, *195*, 113828. [[CrossRef](#)]

Disclaimer/Publisher’s Note: The statements, opinions and data contained in all publications are solely those of the individual author(s) and contributor(s) and not of MDPI and/or the editor(s). MDPI and/or the editor(s) disclaim responsibility for any injury to people or property resulting from any ideas, methods, instructions or products referred to in the content.